

INTI INTERNATIONAL UNIVERSITY

FACULTY OF ENGINEERING AND QUANTITY SURVEYING

**SEISMIC RETROFITTING OF
DEFICIENT RC BEAM-COLUMN JOINT REGIONS
USING PRE-TENSIONED STEEL STRAPS**

**KENNETH BOO BENG WEE
B.ENG (HONS) IN CIVIL ENGINEERING**

PROJECT SUPERVISOR: LEE HOONG PIN

FINAL YEAR PROJECT

2018

SUPERVISOR'S DECLARATION

This project report entitled "Seismic Retrofitting Of Deficient RC Beam-Column Joint Regions Using Pre-tensioned Steel Straps" is prepared and submitted by Kenneth Boo Beng Wee, I14006681 as partial fulfilment of the requirement for Bachelor of Engineering (HONS) in Civil Engineering, INTI International University.


APPROVED BY:


.....
LEE HOONG PIN
Faculty of Engineering and QS
INTI International University
71800 Nilai N. Sembilan
E: hoongpin.lee@newinti.edu.my


Date ... 4 May 2018

STUDENT'S DECLARATION

I hereby declare that the final year project is based on my original work except for quotations and citations, which have been duly acknowledged. I also declare that it has not been previously or concurrently submitted for any other degree at INTL INTERNATIONAL UNIVERSITY or other institutions.

Signature : 

Student Name : .. Kenneth Bao Beng Wee

Student ID : .. I14006681

Date : .. 4 May 2018

ACKNOWLEDGMENT

First and foremost, I would like to express my sincere gratitude to my parents for their endless support and encouragement shown from the start of my final year project, all the way to its completion. Besides, I would like to specifically thank Mr. Lee Hoong Pin, my project supervisor, for the valuable knowledge he shared and for the great generosity demonstrated in allowing me to use the materials belonging to him. It would certainly be impossible to complete this project without his essential guidance. Last but not least, I would also like to thank these friends of mine: Kiew Jie Fu, Keshantran, Lee Wei Sheng, Ahmed Ihusan, and Hassan, for their kind assistance with the lab works. Given that the workload of this project is relatively huge, with the short amount of time provided, it would have been impossible to complete this project if it is not for their assistance.

ABSTRACT

This research presents the study of the seismic performance of deficient RC L-joints confined with pre-tensioned steel straps. The main experimental result parameters investigated are the load applied-drift ratio relationship; ductility; and energy dissipation capacity. Besides, the different corresponding modes of failure of the specimens were properly understood as well. An extensive study was done to review other related journals which will help facilitate a more comprehensive understanding for the outcomes of this research (in Chapter 2). As for this research, 15 RC L-joint specimens with different volumetric ratio of confinement (control; 1 to 4 layers of steel straps) were fabricated and tested under simulated seismic loadings whereby uniaxial cyclic loadings were applied on the specimens' beam tip and column top face. The experimental findings may be summarized as follows: The highest percentage of shear strength enhancement is 40% as that shown by the specimens confined with two layers of steel straps. It was also found that the specimens with high volumetric ratio of confinement have lower rate of stiffness degradation. On the other hand, the highest average displacement ductility factor enhancement (74%) was shown by the specimen group with three layers of steel straps. The energy dissipation capacities of the specimens were found to steadily rise with the increased in volumetric ratio of confinement; the optimum volumetric ratio of confinement for maximum energy dissipation capacity (274%) is 4 layers. Besides, it was shown that with the increased in volumetric ratio of confinement, the mode of failure transitions from brittle-shear to flexural-shear; and then finally to ductile-flexural failure. In general terms, as for the retrofitted RC joint specimens, the main governing parameters behind their enhanced seismic performance are their ductility and energy dissipation capacity.

TABLE OF CONTENTS

CHAPTER	TITLE	PAGES
	DECLARATION	ii - iii
	ACKNOWLEDGEMENT	iv
	ABSTRACT	v
	TABLE OF CONTENTS	vi - ix
	LIST OF FIGURES	x - xviii
	LIST OF TABLES	xix - xx
1	INTRODUCTION	1
	1.1 General	1 - 2
	1.2 Statement of the Problem	3
	1.3 Research Objectives	4
	1.4 Scope of Study	4
	1.5 Significance of Study	5
2	LITERATURE REVIEW	6
	2.1 Introduction	6 - 7
	2.1.1 Seismic retrofitting background	7 - 8
	2.1.2 Common challenges encountered	9 - 10
	2.2 Retrofitting classification	10 - 11
	2.3 Seismic demand for RC beam-column joint regions	11 - 12

2.3.1 Common types of RC beam-column joints	12 - 13
2.3.2 The different types of forces experience by beam-column joints	13 - 16
2.3.3 Seismic behaviour of deficient RC beam-column joints	16 - 19
2.4 Common types of retrofitting techniques for RC beam-column joints	19
2.4.1 Steel Jacketing & Haunch Element by Dang and Dinh (2017)	20 - 24
2.4.2 Fiber Reinforced Polymers (FRP) by Kabir and Hejabi (2015); Ghobarah and Said (2001)	25 - 31
2.4.3 Pre-stressed steel straps by Moghaddam and Samadi (2009); Lopez et al. (2012)	31 - 43
2.4.4 General conclusion on the different retrofitting techniques discussed	44 - 45
2.5 Conclusion	46 - 47
3 METHODOLOGY	48
3.1 Introduction	
3.2. Test specimen design	49
3.2.1 Frame modelling	49 - 50
3.2.2 Addition of load on structural model	51 - 54
3.2.3 Load combination & Structural analysis	55 - 56
3.2.4 Reinforced concrete design per BS8110	57 - 64
3.2.5 Test specimen geometry and detailing specification	64 - 66
3.3 Formwork	66 - 67
3.4 Reinforcement steel bars	68 - 69
3.5 Concrete	70
3.5.1 Concrete mix design	70 - 74
3.5.2 Casting of concrete	75 - 76
3.6 Pre-tensioned Steel Straps	77
3.6.1 Mechanism of pre-tensioned steel straps to the	77 - 78

	joint specimens	
	3.6.2 Steel straps configuration and volumetric ratio of confinement	79 - 80
	3.7 Experimental set-up, specimen loading configuration & data to be collected	81 - 83
	3.8 Overall flow cart for the fabrication and testing of specimen	84 - 85
4	RESULTS AND DISCUSSION	86
	4.1 Introduction	86 - 87
	4.2 Concrete compressive strength	87 - 88
	4.3 Analytical approaches employed in obtaining the experimental result parameters	89
	4.3.1 Specimens' shear strength and stiffness properties	89
	4.3.2 Specimens' displacement ductility factor	90
	4.3.3 Specimens' energy dissipation capacity	90 - 92
	4.4 Control specimens' observation and discussion	93
	4.4.1 Load applied-drift ratio relationship	93 - 97
	4.4.2 Cracking pattern and the mode of failure	98 - 99
	4.5 Specimens confined with one layer of steel strap's observation and discussion	99
	4.5.1 Load applied-drift ratio relationship	99 - 104
	4.5.2 Cracking pattern and the mode of failure	104-105
	4.6 Specimens confined with two layers of steel straps' observation and discussion	106
	4.6.1 Load applied-drift ratio relationship	106-110
	4.6.2 Cracking pattern and the mode of failure	111
	4.7 Specimens confined with three layers of steel straps' observation and discussion	112
	4.7.1 Load applied-drift ratio relationship	112-116
	4.7.2 Cracking pattern and the mode of failure	117-118
	4.8 Specimens confined with four layers of steel straps'	118

observation and discussion	
4.8.1 Load applied-drift ratio relationship	118-123
4.8.2 Cracking pattern and the mode of failure	123-124
4.9 Comparison	125
4.9.1 Shear strength & mode of failure and the load applied-drift ratio relationship	125-129
4.9.2 Ductility and energy dissipation capacity	129-132

5

CONCLUSIONS AND RECOMMENDATIONS

	133
5.1 Summary of study	133-134
5.2 Recommendations for future study	135

REFERENCES

136-138

LIST OF FIGURES

	DESCRIPTION	PAGE
Figure 2.1:	Types of beam-column joints (Uma, 2015)	13
Figure 2.2:	Forces and bending moments acting on an interior joint under different loading (Uma, 2015)	14
Figure 2.3:	Forces and bending moments acting on exterior joints under different detailing (Uma, 2015)	14
Figure 2.4:	Forces and bending moments acting on corner joints (Uma, 2015)	15
Figure 2.5:	Some of the beam-column joint specimens (exterior) (Pampanin et al., 2002)	17
Figure 2.6:	Exterior tee joints- variation in failure mechanism (Pampanin et al., 2002)	19
Figure 2.7:	Specimens' detailing and retrofitting configuration (Dang and Dinh, 2017)	21
Figure 2.8:	Experimental set-up (Dang and Dinh, 2017)	22
Figure 2.9:	Specimens' lateral force versus drift ratio relationship (Dang and Dinh, 2017)	23
Figure 2.10:	Strain profiles of top and & bottom rebars (Dang and Dinh, 2017)	24
		26

Figure 2.11:	Specimen detailing and FRP configuration (Kabir and Hejabi, 2015)	26
Figure 2.12:	Lateral load versus displacement curves (Kabir and Hejabi, 2015)	28
Figure 2.13:	Specimen's detailing & FRP configuration (Ghobarah and Said, 2001)	29
Figure 2.14:	Loading history (Ghobarah and Said, 2001)	29
Figure 2.15:	Load versus displacement curve of the control specimen (left) and the repaired and FRP retrofitted specimen (right) (Ghobarah and Said, 2001)	30
Figure 2.16:	Retrofitting to eliminate joint shear failure (Ghobarah and Said, 2001)	31
Figure 2.17:	Confining action by FRP (Benzaid and Mesbah, 2014)	32
Figure 2.18:	Effective confinement area for different concrete cross-sectional shape (Parvin and Brighton, 2014)	33
Figure 2.19:	Specimen detailing & configuration (Moghaddam and Samadi, 2009)	36
Figure 2.20:	Hysteretic lateral behaviour of specimens (C3–C6) (Moghaddam and Samadi, 2009)	38
Figure 2.21:	Difference in strip strain values with respect to their height position in specimen C4 (Moghaddam and Samadi, 2009)	38
Figure 2.22:	(a) plan view, and (b) geometry of building and members (Lopez et al., 2012)	41
Figure 2.23:	Deficient beam-column joint detailing of (a) 1 st floor (b) 2 nd floor, in the X direction (Lopez et al., 2012)	42
Figure 2.24:	Pre-stressed steel straps strengthening of (a) 1A-1 joint, & (b) 1A-2 joint (Lopez et al., 2012)	42
Figure 2.25:	(a) 1A-2 joint during the Stage 2 test; and (b) 1A-1 joint after the removal of pre-stressed steel straps (Lopez et al., 2012)	43

Figure 3.1:	Frame modelling with Autodesk Robot Structural Analysis Professional 2018	49
Figure 3.2:	Assignment of material and section properties	50
Figure 3.3:	Assignment of support/boundary condition	50
Figure 3.4:	Characteristic dead load	52
Figure 3.5:	Characteristic live load	52
Figure 3.6:	Wind load case 1	53
Figure 3.7:	Wind load case 2	53
Figure 3.8:	Wind load case 3	54
Figure 3.9:	Wind load case 4	54
Figure 3.10:	Load case code combinations options- Autodesk Robot Structural Analysis 2018	55
Figure 3.11:	Full list of load case combinations as per BS8110	56
Figure 3.12:	Analysis type option & performance of structural analysis	56
Figure 3.13:	RC design performed by Autodesk Robot Structural Analysis Professional 2018	57
Figure 3.14:	RC design as per BS8110 and list of load cases included (for beam & column)	58
Figure 3.15:	Example list of ultimate bending moments and axial forces for different load case combinations in column calculation	58
Figure 3.16:	Column RC design calculation results	59
Figure 3.17:	Column RC design calculation results	59
Figure 3.18:	Column section drawing and detailing generated	60
Figure 3.19:	Column 3D view	60

Figure 3.20:	Beam RC design calculation results	61
Figure 3.21:	Beam RC design calculation results	62
Figure 3.22:	Beam RC design calculation results	63
Figure 3.23:	Beam section drawing and detailing generated	63
Figure 3.24:	Beam 3D view	64
Figure 3.25:	Specimen geometry and detailing (units: mm)	65
Figure 3.26:	Section A-A (units: mm)	65
Figure 3.27:	Section B-B (units: mm)	65
Figure 3.28:	Formwork plan (Top view) per specimen	66
Figure 3.29:	Plywood material	67
Figure 3.30:	Mechanical table wood cutter	67
Figure 3.31:	Plywood pieces	67
Figure 3.32:	Hammer & Nails	67
Figure 3.33:	Assembling of formwork	67
Figure 3.34:	Application of sealant	67
Figure 3.35:	Cutting steel bars to appropriate length	68
Figure 3.36:	Bending T12 steel bars	68
Figure 3.37:	Bending R6 (links)	69
Figure 3.38:	Mild steel wire & Cable tie (for tying bars)	69
Figure 3.39:	Example of assembled rebars	69
Figure 3.40:	Rebars in formwork	69

Figure 3.41:	Spacer block (30mm height)	69
Figure 3.42:	Specimens pre-concreting	69
Figure 3.43:	Graph of compressive strength versus water/cement ratio	71
Figure 3.44:	Approximated wet density of fully compacted concrete	72
Figure 3.45:	Mass measurement for sample 1 (example)	73
Figure 3.46:	Sieving sand samples	73
Figure 3.47:	Recommended proportions of fine aggregate as per % passing 600 μ m sieve	74
Figure 3.48:	(a) Portland Cement MS EN 197-1:2014 (Class 42.5) (b) Course aggregates (Max size = 20mm) (c) Fine aggregates/Sand	75
Figure 3.49:	(a) Lubrication of formworks (b) Measuring out concrete constituents (c) Concrete mixing with a mixer	76
Figure 3.50:	(a) Vibrating the concrete mix (b) 24 hours concrete curing outside the water tank	76
Figure 3.51:	(a) Striking formwork (b) Concrete curing inside the water tank	76
Figure 3.52:	Schematic diagram for the pre-tensioning of steel straps (Moghaddam and Samadi, 2009)	78
Figure 3.53:	Pre-tensioning of steel straps/Installation of steel straps unto the specimen	78
Figure 3.54:	Pre-tensioned steel straps configuration	79
Figure 3.55:	Pre-tensioned steel straps retrofitted specimens	79
Figure 3.56:	Control & retrofitted specimens	80
Figure 3.57:	Experimental set-up schematic diagram	82

Figure 3.58:	Experiment set-up	83
Figure 3.59:	Experimental data compilation with the software "OpenShot"	83
Figure 3.60:	Overall flow chart for the fabrication and testing of specimens (1)	84
Figure 3.61:	Overall flow cart for the fabrication and testing of specimens (2)	85
Figure 4.1:	Compressive test machine results for concrete cube sample 1, 2 & 3	88
Figure 4.2:	(a) Concrete compression test (b) Concrete cube (post-compressive test)	88
Figure 4.3:	Graph of "load versus drift ratio" for the 1 st load cycle of specimen 1-C	91
Figure 4.4:	Graph of "load versus drift ratio" for the 2 nd load cycle of specimen 1-C	92
Figure 4.5:	Graph of "load applied versus drift ratio" for specimen 1-C	94
Figure 4.6:	Envelope curve for specimen 1-C	95
Figure 4.7:	Graph of "load applied versus drift ratio" for specimen 2-C	95
Figure 4.8:	Envelope curve for specimen 2-C	96
Figure 4.9:	Graph of "load applied versus drift ratio" for specimen 3-C	96
Figure 4.10:	Envelope curve for specimen 3-C	97
Figure 4.11:	(a) Diagonal crack lines originating at the joint core of specimen 3-C (b) Specimen 3-C post-failure	98
Figure 4.12:	Specimen 2-C post-failure	99
Figure 4.13:	Graph of "load applied versus drift ratio" for specimen 4-	101